OncoTargets and Therapy Dovepress

Open Access Full Text Article ORIGINAL RESEARCH

Cytotoxic Evaluation, Molecular Docking, Molecular Dynamics, and ADMET Prediction of Isolupalbigenin Isolated from *Erythrina subumbrans* (Hassk). Merr. (Fabaceae) Stem Bark: Unveiling Its Anticancer Efficacy

Tati Herlina[1], Abd Wahid Rizaldi Akili[1], Vicki Nishinarizki[1], Ari Hardianto[1], Allyn Pramudya Sulaeman[1], Shabarni Gaffar[1], Euis Julaeha[1], Tri Mayanti[1], Unang Supratman[1,2], Mohd Azlan Nafiah[3], Jalifah Binti Latip[4]

[1]Department of Chemistry, Faculty of Mathematics and Natural Science, Universitas Padjadjaran, Sumedang, West Java, 45363, Indonesia; [2]Central Laboratory, Universitas Padjadjaran, Sumedang, 45363, Indonesia; [3]Department of Chemistry, Faculty of Science and Mathematics, Sultan Idris Education University, Tanjong Malim, Perak, 35900, Malaysia; [4]Department of Chemical Sciences, Faculty of Science and Technology, Universiti Kebangsaan Malaysia (UKM), Bangi, Selangor, 46300, Malaysia

Correspondence: Tati Herlina, Email tati.herlina@unpad.ac.id

Introduction: *Erythrina subumbrans*, a medical plant found in sub-Saharan Africa and the Western Ghats of India, shows promise as a potential source of bioactive compounds to treat cancer. In our ongoing research on folk medical plants, we report the isolation of flavonoid compound from the stem bark of *E. subumbrans* along with its cytotoxic activity against breast cancer (MCF-7 and T47D), and cervical cancer (HeLa) cell lines.

Purpose: This study aimed to isolate secondary metabolite from the stem bark of *E. subumbrans* and evaluate its cytotoxic activity to support the use of folk medicinal plants as alternative therapy against cancer.

Methods: Isolupalbigenin was isolated from the stem bark of *E. subumbrans* by column chromatography. Cytotoxic activity against breast cancer (MCF-7 and T47D) and cervical cancer (HeLa) cell lines was evaluated using the MTT assay, whereas the in silico study was evaluated using molecular docking and molecular dynamics against estrogen receptor alpha (ERα).

Results: The cytotoxic assay showed that isolupalbigenin inhibited the growth of MCF-7 cell with an IC_{50} of 31.62 $\mu g \cdot mL^{-1}$, while showing no toxicity against normal human cells (Vero cell line). The molecular docking results suggested that isolupalbigenin can bind to ERα with a lower binding affinity than estradiol, whereas the stability of the isolupalbigenin-ERα complex was confirmed by molecular dynamic simulation with a median Root Mean Square Deviation (RMSD) of 2.80 Å. Toxicity prediction suggested that isolupalbigenin was less likely to cause hepatotoxicity or carcinogenicity, whereas pharmacokinetic prediction suggested that isolupalbigenin has high intestinal absorption with medium Caco2 permeability. In addition, isolupalbigenin was predicted to have a medium volume of distribution (Vd).

Conclusion: Isolupalbigenin isolated from the stem bark of *E. subumbrans* with cytotoxic activity supports further development of plants from the genus *Erythrina* as a medicinal plant for alternative therapy against cancer.

Keywords: *Erythrina subumbrans*, isolupalbigenin, cytotoxic, in vitro, in silico

Introduction

Cancer is a complex disease that occurs when changes in genes cause cells to grow and proliferate rapidly, leading to a rapid increase in tissue mass in the affected body parts.[1] Its prevalence has surged over the years, making it a leading cause of morbidity and mortality worldwide. The prevalence of cancer varies across regions and countries, with diverse factors contributing to its incidence and impact. The Global Cancer Statistics 2020 report estimated approximately

Received: 19 August 2024
Accepted: 4 October 2024
Published: 17 October 2024

19.3 million new cancer cases and 10 million cancer-related deaths worldwide, highlighting the substantial toll of this disease on public health.[2] Owing to the increasing prevalence of cancer worldwide, it is imperative to explore novel approaches to its prevention and treatment. One such approach involves the use of natural products, particularly flavonoids, which have garnered attention owing to their potential anti-cancer properties.[3,4]

Flavonoids are a class of polyphenolic compounds found in various fruits, vegetables, and plant-derived products. They have been the subject of extensive research because of their diverse biological activities, including antioxidant, anti-inflammatory, and anticancer effects.[5] Epidemiological studies have indicated that dietary intake of flavonoids is associated with a reduced risk of certain types of cancer, suggesting their potential role in cancer prevention.[6] The potential use of flavonoids as anti-cancer agents is supported by their ability to modulate various cellular processes involved in cancer development and progression. Flavonoids have been shown to exhibit cytotoxic effects on cancer cells, induce apoptosis, and inhibit cancer cell proliferation, thereby impeding tumor growth.[7]

Erythrina is a medicinal plant rich in flavonoids is the plants of genus *Erythrina*.[8] *Erythrina subumbrans* is a plant species of the genus *Erythrina* with significant ethnomedical use in sub-Saharan Africa and the Western Ghats of India. The plant has been traditionally utilized to treat various ailments, including parasitic and microbial diseases, inflammation, cancer, and wounds, and as an anthelmintic and antioxidant agent.[9–12] The aqueous ethanolic extract of *E. subumbrans* was reported to have cytotoxic activity against the Human Melanoma cell line (A375) with an IC_{50} of 82.14 μg/mL,[13] which further supports the potency of *E. subumbrans* as a source of flavonoids with cytotoxic activity.

Isolupalbigenin is a natural derived flavonoid that exhibited cytotoxic activities against lung cancer, colorectal cancer, leukemia.[14] This particular flavonoid has been identified in *E. poeppigiana*.[15] As part of our continuing investigation on folk medicinal plants, we report the isolation of flavonoid compound, Isolupalbigenin from the stem bark of *E. subumbrans* along with its cytotoxic activity against breast cancer (MCF-7 and T47D), and cervical cancer (HeLa) cell lines.

Materials and Methods

General Experimental Procedures

UV spectra were measured using a UV-1800 Shimadzu spectrophotometer. IR spectra (KBr disks, in cm^{-1}) were recorded on a One Perkin Elmer Spectrum FTIR spectrometer. HRTOFMS data were obtained on Waters Xefo QTOF spectrometer. NMR spectra were recorded on a JEOL ECZ-500 spectrometer at 500 MHz for ^{1}H and 125 MHz for ^{13}C, using tetramethylsilane (TMS) as an internal standard. Column chromatography (CC) was performed using silica gel G60 (70–230 mesh, Merck). The fractions were monitored thin-layer chromatography (TLC) on silica gel plates (60 F254 plates, Merck). The spots were visualized under UV light (Vilber Lourmat at $\lambda = 254$ and 365 nm) by spraying with 10% aluminium chloride reagent, followed by heating.

Plant Materials

The stem bark of *E. subumbrans* (Hassk). Merr. were collected in July 2019 from the Subang District, West Java Province, Indonesia. A voucher herbarium specimen of *E. subumbrans* (No. 502/HB/05/2019) was deposited in the Plant Taxonomy Laboratory, Department of Biology, Universitas Padjadjaran, Indonesia and was formally identified by botanist Joko Kusmoro.

Extraction and Isolation

Stem bark powder of *E. subumbrans* (3.0 kg) was extracted with methanol at room temperature, followed by concentration under reduced pressure. The resulting concentrated methanol extract (152.56 g) was partitioned successively with n-hexane and ethyl acetate (EtOAc). The EtOAc extract (10.21 g) was separated by column chromatography (CC) on silica gel, employing a gradient solvent system of n-hexane–EtOAc–MeOH, with increasing proportions of polar solvent. This process yielded ten fractions (A–J). Fraction E (1.19 g) was further subjected to CC using an isocratic system of n-hexane: methylene chloride: acetone (2.5:7:0.5), resulting in 10 fractions (E.1–10), which were monitored by thin-layer chromatography (TLC). Fraction E3 was further separated by CC, eluted using a gradient system of n-hexane: chloroform, and purified using an octadecylsilane (ODS) system with MeOH: H_2O (99:1). This process yielded compound 1 (6.2 mg).

Efficacy Cytotoxic Activity Assay

Cytotoxic activity against MCF-7, T47D breast cancer, and HeLa cervical cancer cell lines was assessed using a 3-[4,5-dimethylthiazole-2-yl]-2,5-diphenyltetrazolium bromide (MTT) assay.[16] The cell lines MCF-7 (ATCC, HTB22), T47D (ATCC, HB133), HeLa (ATCC, CCL-2), and Vero (used as a normal control), were sourced from the Faculty of Medicine Research Center at the Universitas Gajah Mada, Yogyakarta, Indonesia. The treated cell culture (1×10^4 cells) was placed in 96-well microplates and incubated in a 5% CO_2 environment at 37°C. After a 24-hour incubation period, varying concentrations of compound 1 (ranging from 15.62–1000 µg/mL) were added to each well and incubated for 48 h. The culture medium served as the negative control, and doxorubicin (DOX) was used as the positive control. After incubation, the supernatant was discarded and the wells were rinsed twice with phosphate-buffered saline (PBS). Subsequently, 100 µL of 0.5 mg/mL MTT was added to each well and incubated for 4–6 h at 37°C in a 5% CO_2 environment. A stopper solution containing 10% sodium dodecyl sulfate (SDS) was added to dissolve formazan crystals. Absorbance was measured at 595 nm using a Bio-Rad Benchmark microplate absorbance reader. The cytotoxic activity was expressed as the IC_{50} value, which was calculated using a linear regression equation.

Molecular Docking & Molecular Dynamics Simulation

The 3D X-ray crystal structure of the estrogen receptor alpha (ERα) ligand–binding domain was retrieved from the Protein Data Bank (PDB) (https://www.rscb.org, accessed on 09 December 2023) with PDB ID of 3ERT. The protein and co-crystallized ligand were extracted and individually saved as pdb files using the Biovia Discovery Studio (DS) 2021 Client software. Subsequently, the protein and co-crystallized ligand were prepared for re–docking using AutoDockTools 1.5.6. Both the processed protein and ligand structures were saved in the pdbqt format. Protein and ligand structures were docked using AutoDock Vina 1.2.3. The root mean square deviation (RMSD) was calculated by superimposing the docked ligand on the original ligand from the crystal structure.

Using Chemaxon MarvinSketch software, the protonated state of compound 1 was predicted at a physiological pH of 7.4. The three-dimensional (3D) structure of compound 1 was then generated and optimized using the MMFF94 force field with Avogadro software, and saved in the pdb format. This 3D structure was processed for molecular docking using AutoDockTools 1.5.6. and saved in the pdbqt format. Subsequently, the structure underwent molecular docking, adhering to the protocol outlined for the redocking process.

The molecular dynamics simulation was performed using the Particle-Mesh Ewald Molecular Dynamics (PMEMD) module within AMBER20, with GPU acceleration. The initial minimization process involved 1000 steps of the steepest descent method and 2000 steps of the conjugate gradient method, with an applied harmonic force of 5 kcal mol^{-1} $Å^{-2}$. This was followed by 5000 steps of unrestricted conjugate gradient minimization to correct for any spatial overlap. The system's temperature was gradually increased to 300 K in increments of 20 ps (0–100 K; 100–200 K; and 200–300 K), taking a total of 60 ps. A period of equilibration was then carried out to ensure consistent density, pressure, and gradual release of force over 1000 ps. Finally, the production runs were carried out for a duration of 100 ns, with each step taking 2 fs.[17]

In silico Toxicity and Pharmacokinetics Prediction

The toxicity and pharmacokinetics of compound 1 were predicted using the pkCSM web server (https://biosig.lab.uq.edu.au/pkcsm/ accessed December 27, 2023). The pkCSM is a freely accessible web server that provides an integrated platform to rapidly evaluate pharmacokinetic and toxicity properties using a graph-based signature to represent small molecules and train predictive models.[18]

Results

Structure Elucidation of Compound 1

Compound 1 was isolated as a pale–yellow amorphous powder. The UV spectrum of compound 1 at acetone solvent (Figure S1) exhibited absorbance peaks of λ_{max} at 325 nm and 287 nm, with log ε values of 3.81 and 2.75, respectively. Both of these absorbances are characteristics of flavonoid compound. Absorbance at λ_{max} of 325 nm indicates the presence of cinnamoyl chromophore system, whereas absorbance at λ_{max} of 287 nm indicates the presence of benzoyl chromophore system. The IR spectrum (Figure S2) revealed characteristic absorption: hydroxyl groups at ν_{max} 3368 cm^{-1}, stretching vibrations of C-H bonds

at v_{max} 2968 and 2913 cm^{-1}, a carbonyl group (ketone) at v_{max} 1651 cm^{-1}, stretching vibrations of C=C (sp^2) bonds at v_{max} 1505 cm^{-1}, stretching vibrations of C-O (ether) bonds at v_{max} 1267 cm^{-1}, and bending vibrations of C-H (aromatic) bonds at v_{max} 829 cm^{-1}. HRTOF-MS: m/z 407.1803 $[M + H]^+$, calculated for $C_{25}H_{26}O_5$ m/z 407.1858 (Figure S3).

The ^{13}C NMR spectrum (Figure S4) reveals 25 carbon signals, comprising: one carbonyl carbon signal at δC 181.1 ppm, four oxygenated sp2 quaternary carbons at δC 161.5, 160.5, 155.3, and 155.1 ppm, one oxygenated sp2 methine carbon at δC 153.4 ppm, six sp2 methine carbons at δC 130.3, 127.6, 122.8, 122.3, 114.6, and 98.5 ppm, seven sp2 quaternary carbons at δC 131.5, 131.1, 127.7, 123.0, 122.2, 106.2, and 105.2 ppm, two sp3 methylene carbons at δC 28.3 and 21.1 ppm, and four sp3 methyl carbons at δC 25.0, 24.9, 17.0, and 17.0 ppm.

The ^1H-NMR spectrum of compound 1 (Figure S5) reveals four singlet signals corresponding to sp3 methyl protons at δH 1.66, 1.71, 1.73, and 1.79 ppm (each with a multiplicity of 3H). Additionally, there are two deshielded doublet signals attributed to sp3 methylene protons at δH 3.36 (2H, d, J = 7 hz) and 3.44 ppm (2H, d, J = 7 hz). Within the spectrum, six signals correspond to sp2 methine protons, with two of them appearing at δH 5.24 (1H, t, J = 7 hz) and 5.38 ppm (1H, t, J = 7 hz), likely associated with protons in the prenyl chain. Four other sp2 methine proton signals occur at δH 6.39 (1H, s), 6.91 (1H, d, J = 8 hz), 7.28 (1H, dd, J = 8; 2 hz), and 7.35 ppm (1H, d, J = 2 hz), suggesting their presence in an aromatic ring. The proton signals at δH 3.36 and 3.44; 5.24; and 5.38 ppm, each with a coupling constant (J) of 7 hz, indicate vicinal positions within the hydrocarbon chain—specifically, H-1", H-1"', H-2"', and H-2". Furthermore, the aromatic ring protons at δH 6.91 and 7.28 ppm, with a J value of 8 hz, correspond to ortho positions (H-5' and H-6'), while those at δH 7.28 and 7.35 ppm, with a J value of 2 hz, suggest meta positions (H-6' and H-2'). Notably, the spectrum includes one signal for an oxygenated methine proton at δH 8.23 ppm (1H, s), characteristic of flavonoids. Meanwhile, there are three singlet signals for protons from hydroxyl groups at δH 8.84, 10.31, and 13.02 ppm. The signal at δH 13.02 ppm is characteristic of the H-5 position in ring A because it can form a chelate with the carbonyl group at position C-4. Based on the NMR spectrum and comparison with data available in the literature, compound 1 was elucidated as Isolupalbigenin. The ^1H NMR (500 MHz, $(CD_3)_2CO$) and ^{13}C NMR (125 MHz, $(CD_3)_2CO$) spectra comparison of compound 1 and Isolupalbigenin from the available literature[19] is shown in Table 1.

Cytotoxic Activity of Compound 1

The anticancer activity of compound 1 was evaluated against three cancer cell lines: MCF-7, T47D, and HeLa. The results showed that compound 1 exerted different effects in different cell lines. Among the three cancer cell lines, isolupalbigenin exhibited the highest cytotoxic activity against MCF-7 cells with an IC_{50} of 31.62 ± 2.86 μg·mL^{-1} (77.79 ± 7.04 μM), followed by T47D and Hela with IC_{50} of 54.17 ± 2.69 μg·mL^{-1} (133.27 ± 6.62 μM), 122.16 ± 5.17 μg·mL^{-1} (300.53 ± 12.72 μM) respectively. The cytotoxic assay was performed using doxorubicin (DOX), a commercial anticancer agent, as the positive control. DOX exhibited significant cytotoxic activity against MCF-7, T47D, and HeLa with IC_{50} of 19.4 ± 1.67 μg·mL^{-1} (35.59 ± 3.08 μM), 0.17 ± 0.03 μg·mL^{-1} (0.31 ± 0.06 μM), and 3.38 ± 0.08 μg·mL^{-1} (6.22 ± 0.14 μM), respectively. Both isolupalbigenin and DOX were also evaluated against the Vero cell line and showed the lowest cytotoxic effect with IC_{50} of 165 ± 11.81 μg·mL^{-1} (405.92 ± 29.05 μM) and 55.35 ± 3.02 μg·mL^{-1} (101.83 ± 5.56 μM).

Molecular Docking and Molecular Dynamics Simulation of Compound 1 Against ERα

According to the cytotoxicity assay, compound 1 exhibited the highest cytotoxic activity against MCF-7 cells. MCF 7 is a human breast cancer cell line with estrogen, progesterone, and glucocorticoid receptors[20] therefore, molecular docking and molecular dynamic simulation of compound 1 were simulated against estrogen receptor alpha (ERα), which is a crucial marker for the cure and prevention of breast cancer.[21] The binding energy obtained from molecular docking showed that 4-hydroxytamoxifen has the lowest binding energy of −9.556 kcal/mol, followed by compound 1 and estradiol with binding energy of −9.148 and −8.965 kcal/mol respectively. In the AutoDock Vina docking score, a more negative value corresponded to a stronger interaction between the ligand and enzyme.[22] Based on the docking score, the binding affinity of compound 1 was weaker than that of 4-hydroxytamoxifen, but stronger than that of estradiol.

Table 1 ^{1}H and ^{13}C NMR Data Comparison of Compound 1 with Isolupalbigenin

Position	Compound 1[a]		Isolupalbigenin[b]	
	δH ppm (ΣH, mult, *J* in Hz)	δC ppm	δH ppm (ΣH, mult, *J* in Hz)	δC ppm
2	8.23 (1H, s)	153.4	7.89 (1H, s)	152,7
3	–	123.0	–	123,4
4	–	181.1	–	181,3
5	–	159.7	–	159,7
6	6.39 (1H, s)	98.5	6.29 (1H, s)	98,9
7	–	161.5	–	161,8
8	–	106.2	–	106,7
9	–	155.3	–	155,4
10	–	105.2	–	105,4
1'	–	122.2	–	122,4
2'	7.35 (1H, d, 2)	130.3	7.20 (1H, d, 2)	130,2
3'	–	127.7	–	127,9
4'	–	155.1	–	154,8
5'	6.91 (1H, d, 8)	114.6	6.85 (1H; d; 8)	115,3
6'	7.28 (1H, dd, 8, 2)	127.6	7.23 (1H; dd; 8; 2)	127,8
1''	3.36 (2H, d, 7)	28.3	3.38 (2H; d; 7)	28,8
2''	5.38 (1H, t, 7)	122.3	5.35 (1H; t; 7)	122,0
3''	–	131.5	–	133,5
4''	1.71 (3H, s)	25.0	1.75 (3H; s)	25,7
5''	1.73 (3H, s)	17.0	1.74 (3H; s)	17,7
1'''	3.44 (2H, d, 7)	21.1	3.43 (2H; d; 6.5)	21,4
2'''	5.24 (1H, t, 7)	122.8	5.22 (1H; tm; 7)	122,0
3'''	–	131.1	–	132,2
4'''	1.66 (3H, s)	24.9	1.69 (3H; s)	25,6
5'''	1.79 (3H, s)	17.0	1.80 (3H; s)	17,8
5-OH	13.02 (1H, s)	–	–	–
7-OH	10.31 (1H, s)	–	–	–
4'-OH	8.84 (1H, s)	–	–	–

Notes: [a]Acetone-*d6*; ^{1}H-NMR 500 MHz; ^{13}C-NMR 125 MHz. [b]$CDCl_3$; ^{1}H-NMR 500 MHz; ^{13}C-NMR 125 MHz.

The RMSD parameter derived from molecular dynamics simulations suggested that the binding of certain ligands can induce relative stabilization of the conformation of Estrogen Receptor alpha (ERα). The most notable effect was demonstrated by 4-hydroxytamoxifen, which decreased the RMSD to a median of 2.18 Å. The interquartile range (IQR), which measures statistical dispersion, is 0.53 Å, indicating that most of the RMSD values of 4-hydroxytamoxifen complex lie within this range. Conversely, estradiol binding also diminished protein RMSD values, resulting in a median of 2.20 Å and an IQR of 1.13 Å. Although binding of isoapulbigenin induces conformational changes in ERα, the stability of the protein remains comparable to that of the apo form. Despite a higher IQR (0.55 Å) compared to the apo form (0.41 Å), its binding reduces RMSD values of ERα to a median of 2.80 Å. In addition, In the root mean square fluctuation (RMSF) of ligand–free and ligand–bound ERα, fluctuations were recorded in the amino acid residues of four specific regions: H3 (R331–R342), H9 (R456–R469), and those surrounding the terminal helix H12 (R523–R535 and R542–R551) (Table 2).

In silico ADMET Prediction of Compound 1

The toxicity prediction of isoapulbigenin suggested that this compound is not carcinogenic and does not cause hepatotoxicity. Although compound 1 is not an inhibitor of hERG I, it can potentially inhibit hERG II, raising concerns regarding its potential impact on cardiac safety.[17] The pharmacokinetic predictions of isoapulbigenin, including its absorption, distribution, metabolism, and excretion properties, are presented in Table 3.

Table 2 The Average RMSF Values for Specific Region of ERα Apoenzyme, Estradiol-ERα Complex, Isolapulbigenin-ERα Complex, 4-Hydroxytamoxifen-ERα Complex Over 100 Ns Time Trajectory

Helices	Residues	Apo	4-hydroxytamoxifen	Estradiol	Isolapulbigenin
H3	R331–R342	2.16	2.78	2.25	2.19
H9	R456–R469	1.60	1.50	1.75	1.62
H12	R523–R535	2.02	2.67	1.46	2.14
H12	R542–R551	3.80	4.89	4.03	2.90

Table 3 Pharmacokinetics Prediction of Compound 1

Property	Parameter	Predicted Value	Unit
Absorption	Water solubility	−5.246	log mol/L
	Caco2 permeability	0.76	log Papp in 10–6 cm/s
	Intestinal absorption	90.488	% Absorbed
	P-glycoprotein substrate	Yes	–
	P-glycoprotein I inhibitor	Yes	–
	P-glycoprotein II inhibitor	Yes	–
Distribution	VDss	−0.139	log L/kg
	Fraction unbound	0.042	Fu
	BBB permeability	−0.993	log BB
	CNS permeability	−1.843	log PS
Metabolism	CYP2D6 substrate	No	–
	CYP3A4 substrate	Yes	–
	CYP1A2 inhibitor	Yes	–
	CYP2C19 inhibitor	Yes	–
	CYP2C9 inhibitor	Yes	–
	CYP2D6 inhibitor	No	–
	CYP3A4 inhibitor	Yes	–
Excretion	Total Clearance	0.353	log mL/min/kg
	Renal OCT2 substrate	No	–

Discussion

Chemical investigation of the ethyl acetate fraction of *E. subumbrans* led to the isolation of Compound 1. The structure of compound 1 was determined based on physical and spectroscopic comparisons with the published literature, and was identified as isolupalbigenin (Figure 1). Isolupalbigenin is natural prenylated isoflavone that has been previously isolated from other medicinal plants, including the bark of *E. poeppigiana*.[15] In addition, this compound has been reported to possess numerous bioactivities, including gastroprotective,[23] α-glucosidase inhibitory, and cytotoxic activities against lung cancer, colorectal cancer, leukemia,[14] and human glyoxalase I.[15]

In our study, the isolated compound, isolupalbigenin, was subjected to a cytotoxic assay against several cancer cell lines, including MCF-7, T47D, and HeLa, as well as a normal cell line. The results showed that isolupalbigenin exhibited the highest activity against the MCF-7 breast cancer cell line, with an IC_{50} value of 31.62 $\mu g \cdot mL^{-1}$ and showed no toxicity towards normal cells, with an IC_{50} of > 150 $\mu g \cdot mL^{-1}$ against the Vero cell line (Figure 2). These data suggested that isolupalbigenin does not harm normal cells, indicating its high selectivity. MCF-7 cells are a well-known human breast cancer cell line that exhibits responsiveness to estrogen owing to the presence of estrogen receptors.[24] Estrogen Receptor (ER) significantly influences the growth, progression, and invasion of ER-expressing breast cancer.[25] Estrogen receptor alpha (ERα) is present in approximately 65% of all breast cancer cases. They promote tumor growth when bound to estrogen, and can prevent cell death by increasing Bcl-2 expression.[26] Considering the importance of ERα in

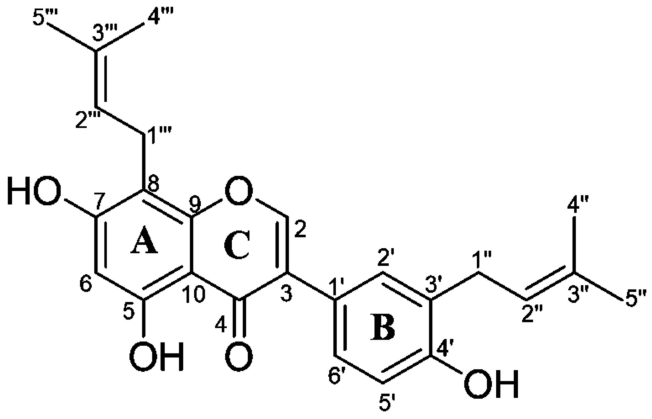

Figure 1 Chemical Structure of Isolupalbigenin.

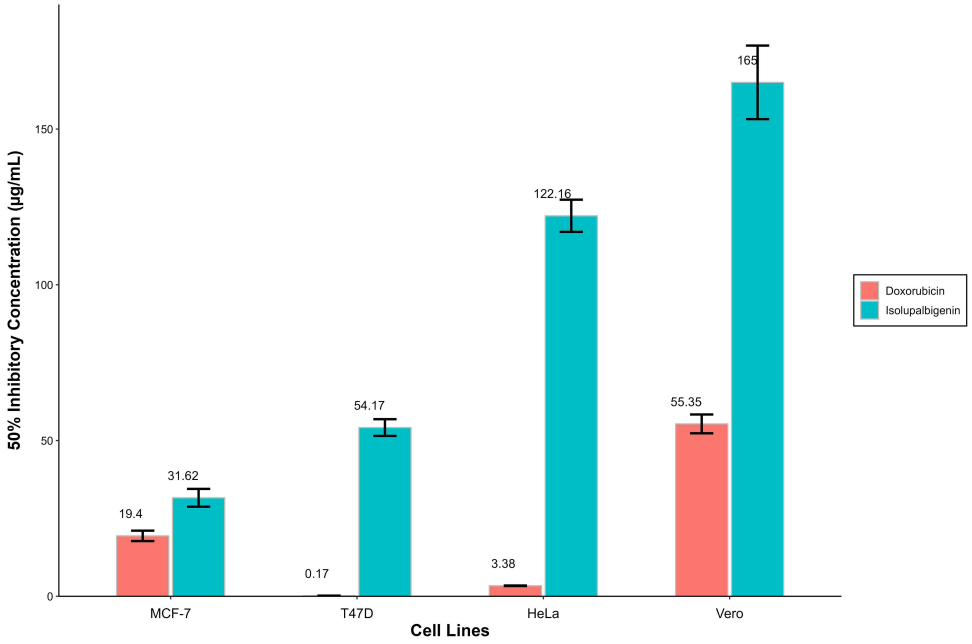

Figure 2 The IC_{50} values (in µM) of compound 1 against several cancer cell lines. Vero cells was used to evaluated the toxicity on normal mammalian cells. DOX was presented as a positive control.

breast cancer cell proliferation, we conducted molecular docking and molecular dynamics simulations to investigate the interaction between isolupalbigenin and ERα.

Molecular docking is a computational technique used to predict the optimal binding conformation and affinity of a small molecule to a protein or receptor. Prior to molecular docking, a redocking procedure was conducted using a complex of Estrogen Receptor alpha (ERα) and 4-hydroxytamoxifen (PDBid 3ERT) to validate the docking protocol. Redocking is a common validation method, in which a known ligand is removed from its receptor and docked back into it. The validity of the docking protocol was assessed by calculating the RMSD between the original and redocked positions of 4-hydroxytamoxifen. RMSD is a measure of the average distance between the atoms of superimposed molecules. If RMSD was < 2 Å (angstroms), the docking protocol was considered valid. The best pose (position and orientation) of 4-hydroxytamoxifen obtained through the redocking procedure had an RMSD of 1.11 Å. This indicated that the molecular docking protocol was valid because this value was less than 2 Å. This successful validation suggests that the protocol is likely to produce reliable results when used to dock other compounds such as isolupalbigenin into

ERα. This process is crucial in the field of drug design as it helps predict the interaction between drugs and their target proteins.

The binding pose (*ie*, the orientation of the ligand when it is bound to the receptor) and binding affinity (*ie*, the strength of the interaction between the ligand and receptor) derived from molecular docking studies provide pivotal information for computer-aided drug design.[27] The binding energy obtained from molecular docking showed that 4-hydroxytamoxifen has the lowest binding energy of −9.556 kcal/mol, followed by isolupalbigenin and estradiol with binding energy of −9.148 and −8.965 kcal/mol respectively. In the AutoDock Vina docking score, a more negative value corresponded to a stronger interaction between the ligand and enzyme.[22] Based on the docking score, the binding affinity of isolupalbigenin was weaker than that of 4-hydroxytamoxifen, but stronger than that of estradiol.

In terms of binding pose, isolupalbigenin forms a hydrophobic interaction with several amino acid residues within the binding pocket of the ERα ligand–binding domain. Hydrophobic interactions are non-polar interactions that occur between non-polar amino acid residues and non-polar regions of the ligand.[28] One of these amino acid residues is leucine 346 (Leu346), which forms an amide–π stacking interaction with the aromatic C ring of isolupalbigenin (Figure 3). Amide-π stacking is a specific type of non-covalent interaction in which the π system of an aromatic ring interacts with the amide group of a protein. This type of interaction is less well understood than aromatic-aromatic stacking, but it plays an important role in protein-ligand binding.[28] Leu346 is considered to be an antiestrogenic residue,[29] indicating that it plays a crucial role in the recognition of antiestrogenic ligands.[30] Antiestrogenic ligands bind to estrogen receptors such as ER, and inhibit their activity.[31] Therefore, the interaction between Leu346 and isolupalbigenin may potentially influence the anti–estrogenic activity of ERα.

Molecular docking is a widely used technique in the field of drug design and discovery owing to its ability to predict potential interactions between the ligand or drug and the target protein or receptor.[32] However, one limitation of molecular docking is that it treats the receptor as rigid, which does not account for the flexibility of the protein–ligand complex.[33] To account for this flexibility, we conducted a 100 nanosecond (ns) molecular dynamics simulation to investigate the conformational aspect and residual flexibility of the protein-ligand complex and the apo-form of ERα.

The RMSD was used to evaluate the degree of constancy of isolupalbigenin, 4-hydroxytamoxifen, and estradiol (Figure 4). The RMSD parameter provides important information about the ligand-protein complex, with a lower RMSD value indicating a greater stability of the complex.[34] In this study, we observed that the binding of certain ligands induced the relative stabilization of the conformation of Estrogen Receptor alpha (ERα). The most notable effect was demonstrated by 4-hydroxytamoxifen, which decreased the RMSD to a median of 2.18 Å. The interquartile range (IQR), which

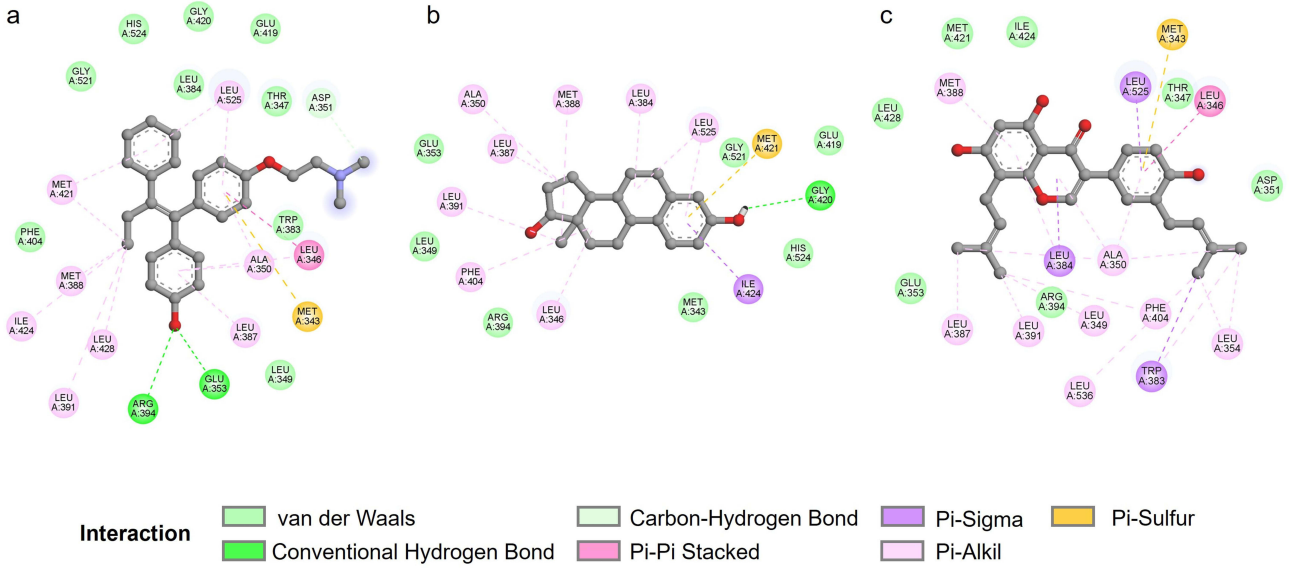

Figure 3 Graphical representation of the interaction between 4-hydroxytamoxifen (**a**), estradiol (**b**), and isolupalbigenin (**c**) with amino acids residue of ERα ligand binding domain.

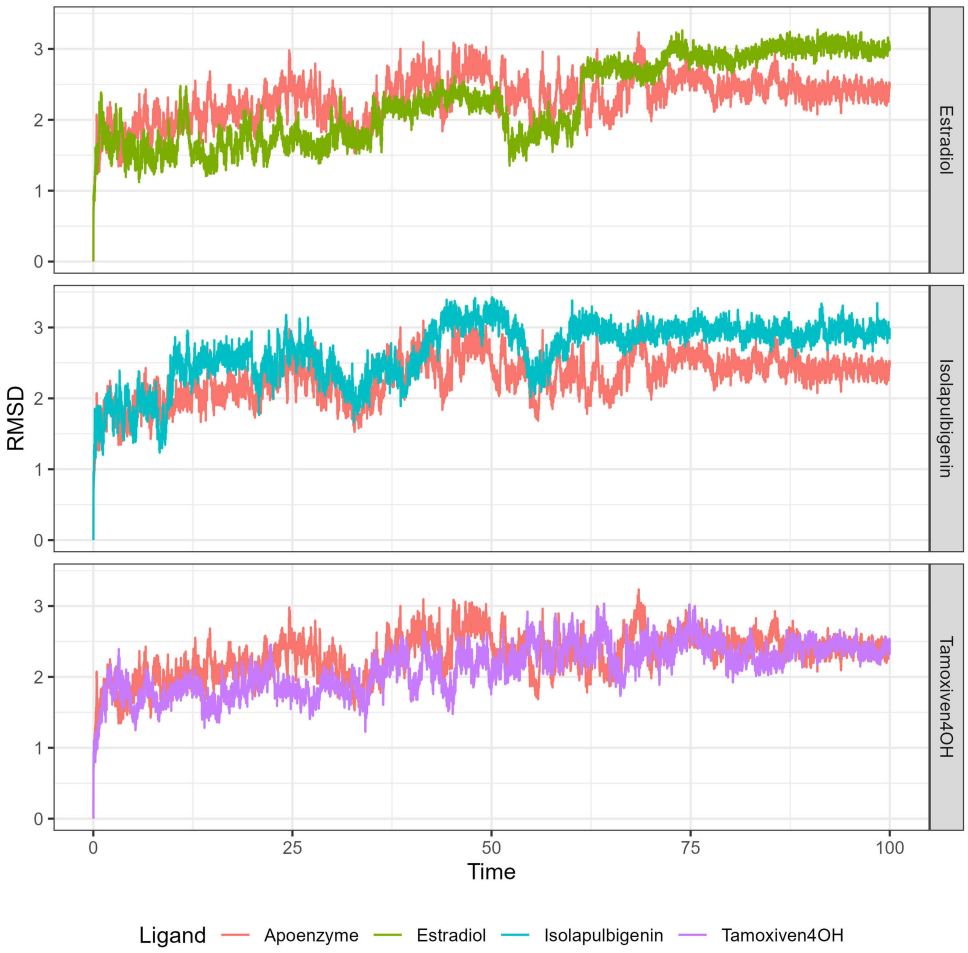

Figure 4 The RMSD plot of ERα apoenzyme, Estradiol-ERα complex, Isolapulbigenin-ERα complex, Tamoxiven-ERα complex over 100 ns time trajectory.

measures statistical dispersion, is 0.53 Å, indicating that most of the RMSD values of 4-hydroxytamoxifen complex lie within this range. Conversely, estradiol binding also diminished protein RMSD values, resulting in a median of 2.20 Å and an IQR of 1.13 Å. Although the binding of isoapulbigenin induces conformational changes in ERα, the stability of the protein remains comparable to that of the apo form. Despite a higher IQR (0.55 Å) compared to the apo form (0.41 Å), its binding reduces RMSD values of ERα to a median of 2.80 Å.

The RMSD and RMSF are two important metrics used in Molecular Dynamics (MD) simulations, that provide different insights into the behavior of molecular structures. While RMSD provides a broad overview of the structural changes in the entire protein over time, RMSF provides a more detailed view, showing the flexibility of the individual amino acids of the protein during the simulation.[17] Higher RMSF values indicate regions of proteins with lower stability and greater flexibility. These regions exhibit dynamic behavior, with a propensity for more pronounced conformational alterations. Conversely, lower RMSF values demonstrate enhanced stability and restricted flexibility, maintaining a relatively invariant structure throughout the simulation.[30]

In the RMSF of ligand-free and ligand-bound ERα (Figure 5), fluctuations were recorded in the amino acid residues of four specific regions: H3 (R331–R342), H9 (R456–R469), and those surrounding the terminal helix H12 (R523–R535 and R542–R551) (Table 2). These regions are part of the ERα protein structure and play crucial roles in ERα function.[35,36] The H12 region is important because it regulates ERα activity by alternating between the active and inactive conformations of this protein.[37,38] This switching mechanism is a common feature of many proteins and is crucial for their function. Interestingly, the highest fluctuation for all systems for both ligand-free and ligand-bound ERα was observed in the terminal H12 region (R542–R551). This suggests that this region may be particularly sensitive to changes in the presence or absence of ligands. However, at R523–R535 in the H12

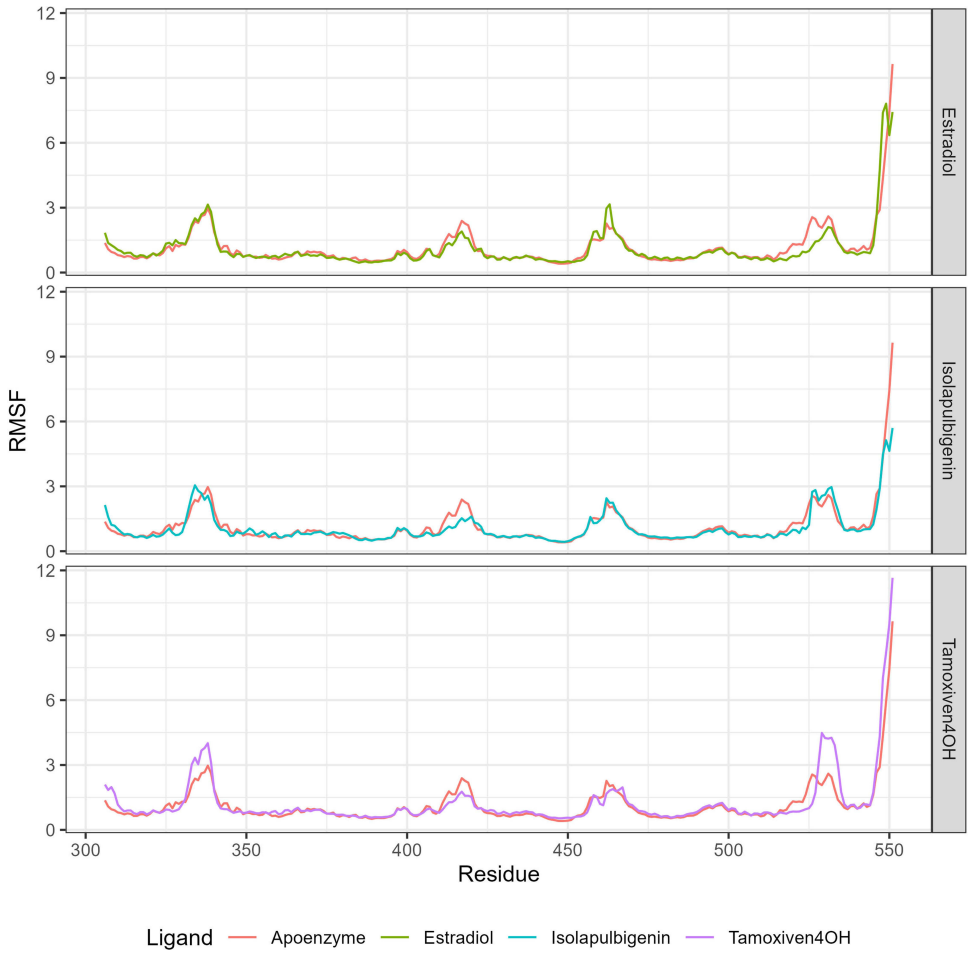

Figure 5 The RMSF plot of ERα apoenzyme, Estradiol-ERα complex, Isolapulbigenin-ERα complex, 4-Hydroxytamoxifen -ERα complex over 100 ns time trajectory.

region, the estradiol-ERα complex showed the least fluctuation compared to the Apo system (ligand-free ERα) and both the 4-hydroxytamoxifen and isolapulbigenin complexes. This observation aligns with a previous study, which found that ERα bound to an antagonist showed more significant structural fluctuations than ERα bound to an agonist.[39] This could be due to the different ways in which agonists and antagonists interact with ERα, leading to different conformational changes in the protein structure.[40,41] Taken together, the results of in vitro and in silico studies indicate that isoapulbigenin could be a potential drug for the treatment of breast cancer. Therefore, in this study, we investigated the toxicity and pharmacokinetic properties of isoapulbigenin.

In terms of potential toxicity to human health, isoapulbigenin was predicted to be non-carcinogenic and non-hepatotoxic, indicating a low potential for toxicity to human health. However, it may also inhibit the expression of hERG II. Pharmacokinetic predictions suggested that isoapulbigenin has medium Caco2 permeability and high intestinal absorption. Nevertheless, being a substrate of P-glycoprotein (P-gp) and its poor water solubility potentially affect the amount absorbed into the body. Despite being predicted to be a substrate of P-gp, isoapulbigenin was also predicted to be an inhibitor of both P-glycoprotein I and II, which prevents these proteins from forcing xenobiotic compounds back into the lumen.[42] In terms of distribution, the prediction suggested that isoapulbigenin was moderately distributed in the tissue than in the plasma, suggesting that lower dosage is required to achieve the desired plasma concentration.[43] Nevertheless, isoapulbigenin has a low unbound fraction, which lowers its efficiency in diffusing through cellular membranes.[17] Moreover, isoapulbigenin may cross the central neural system more easily, but has poor permeability to the blood-brain barrier. In terms of metabolism, The PKCSM prediction suggested that isoapulbigenin may undergo modification by CYP3A4; however, isoapulbigenin was also predicted to inhibit several cytochrome P450 (CYP) enzymes, including

CYP1A2, CYP2C19, CYP2C9, and CYP3A4. In terms of the excretion parameter, the PKCSM prediction suggested that isoapulbigenin has medium total clearance and is not substrate of Renal OCT2.

Conclusion

Isolupalbigenin was successfully isolated from stem bark of *E. subumbrans*. Cytotoxic assay demonstrated that isolupalbigenin can inhibit the growth of the MCF-7 cell line with an IC_{50} of 31.62 µg·mL-1, while exhibiting no toxicity against the normal human cell line, Vero. Molecular docking results suggest that isolupalbigenin can bind to ERα with a lower binding affinity than estradiol. The stability of the isolupalbigenin-ERα complex was confirmed by molecular dynamic simulation, with a median RMSD of 2.80 Å and IQR of 0.55 Å. Toxicity predictions indicated that isolupalbigenin is less likely to cause hepatotoxicity or carcinogenicity. Pharmacokinetics predictions suggest that isolupalbigenin has high intestinal absorption with medium Caco2 permeability and medium volume of distribution. The isolation of isolupalbigenin from the stem bark of *E. subumbrans* which demonstrated cytotoxic activity supports the further development of plants from the *Erythrina* genus as medicinal plants for alternative cancer therapies.

Acknowledgments

The authors are grateful to Universitas Padjadjaran for providing funds through the Academic Leadership Grant (ALG) scheme (No.1608/UN6.3.1/PT.00/2024) by Tati Herlina.

Disclosure

The author(s) report no conflicts of interest in this work.

References

1. Anand U, Dey A, Chandel AKS, et al. Cancer chemotherapy and beyond: current status, drug candidates, associated risks and progress in targeted therapeutics. *Genes Dis*. 2023;10(4). doi:10.1016/j.gendis.2022.02.007
2. Sung H, Ferlay J, Siegel RL, et al. Global cancer statistics 2020: GLOBOCAN estimates of incidence and mortality worldwide for 36 cancers in 185 countries. *CA Cancer J Clin*. 2021;71(3):209–249. doi:10.3322/caac.21660
3. Tuli HS, Garg VK, Bhushan S, et al. Natural flavonoids exhibit potent anticancer activity by targeting microRNAs in cancer: a signature step hinting towards clinical perfection. *Transl Oncol*. 2023:27. doi:10.1016/j.tranon.2022.101596.
4. Kopustinskiene DM, Jakstas V, Savickas A, Bernatoniene J. Flavonoids as anticancer agents. *Nutrients*. 2020;12(2):457. doi:10.3390/nu12020457
5. Forni C, Rossi M, Borromeo I, et al. Flavonoids: a myth or a reality for cancer therapy? *Molecules*. 2021;26(12):3583. doi:10.3390/molecules26123583
6. Wang M, Yu F, Zhang Y, Chang W, Zhou M. The effects and mechanisms of flavonoids on cancer prevention and therapy: focus on gut microbiota. *Int J Biol Sci*. 2022;18(4). doi:10.7150/ijbs.68170
7. Dobrzynska M, Napierala M, Florek E. Flavonoid nanoparticles: a promising approach for cancer therapy. *Biomolecules*. 2020;10(9):1268. doi:10.3390/biom10091268
8. Fahmy NM, Al-Sayed E, El-Shazly M, Singab AN. Comprehensive review on flavonoids biological activities of Erythrina plant species. *Ind Crops Prod*. 2018;123:500–538. doi:10.1016/j.indcrop.2018.06.028
9. Kone WM, Solange KNE, Dosso M. Assessing sub-saharian Erythrina for efficacy: traditional uses, biological activities and phytochemistry. *Pak J Biol Sci*. 2011;14(10):560–571. doi:10.3923/pjbs.2011.560.571
10. Ganesh S, Vijey Aanandhi M. Erythrina subumbrans (Hassk) Merr: an overview. *Int J Res Pharmaceut Sci*. 2020;11(SPL4). doi:10.26452/ijrps.v11ispl4.4232
11. Ganesh S, Vijey Aanandhi M. Anthelmintic and antioxidant activity of aqueous ethanolic extract of Erythrina subumbrans (Hassk.) Merr. *Int J Res Pharmaceut Sci*. 2020;11(SPL4). doi:10.26452/ijrps.v11ispl4.4511
12. Rukachaisirikul T, Innok P, Aroonrerk N, et al. Antibacterial pterocarpans from Erythrina subumbrans. *J Ethnopharmacol*. 2007;110:171–175. doi:10.1016/j.jep.2006.09.022
13. Ganesh S, Vijey Aanandhi M. In-vitro cytotoxic activity of papaverine compound isolated from aqueous ethanolic leaf extract of Erythrina subumbrans (Hassk.) Merr. *Int J Res Pharmaceut Sci*. 2021;12(2). doi:10.26452/ijrps.v12i2.4698
14. Suthiphasilp V, Rujanapun N, Kumboonma P, et al. Antidiabetic and cytotoxic activities of rotenoids and isoflavonoids isolated from Millettia pachycarpa Benth. *ACS Omega*. 2022;7(28):24511–24521. doi:10.1021/acsomega.2c02163
15. Hikita K, Tanaka H, Murata T, et al. Phenolic constituents from stem bark of Erythrina poeppigiana and their inhibitory activity on human glyoxalase I. *J Nat Med*. 2014;68(3):636–642. doi:10.1007/s11418-014-0834-z
16. Salma shaik, N Harikrishnan. Evolution of cytotoxicity of the phytopigments isolated from Spirulina platen sis using MTT assay. *J Popul Ther Clin Pharmacol*. 2023;30(4). doi:10.47750/jptcp.2023.30.04.033
17. Hardianto A, Mardetia SS, Destiarani W, Budiman YP, Kurnia D, Mayanti T. Unveiling the anti-cancer potential of onoceranoid triterpenes from Lansium domesticum Corr. cv. kokosan: an in silico study against estrogen receptor alpha. *Int J Mol Sci*. 2023;24(19):15033. doi:10.3390/ijms241915033

18. Pires DEV, Blundell TL, Ascher DB. pkCSM: predicting small-molecule pharmacokinetic and toxicity properties using graph-based signatures. *J Med Chem*. 2015;58(9):4066–4072. doi:10.1021/acs.jmedchem.5b00104
19. Queiroz EF, Atindehou KK, Terreaux C, Antus S, Hostettmann K. Prenylated Isoflavonoids from the root bark of Erythrina vogelii. *J Nat Prod*. 2002;65(3):403–406. doi:10.1021/np0103867
20. Prayogo AA, Wijaya AY, Hendrata WM, et al. Dedifferentiation of MCF-7 breast cancer continuous cell line, development of breast cancer stem cells (BCSCs) enriched culture and biomarker analysis. *Indonesian Biomed J*. 2020;12(2):115–123. doi:10.18585/inabj.v12i2.977
21. Muhammad S, Saba A, Khera RA, et al. Virtual screening of potential inhibitor against breast cancer-causing estrogen receptor alpha (ERα): molecular docking and dynamic simulations. *Mol Simul*. 2022;48(13):1163–1174. doi:10.1080/08927022.2022.2072840
22. Xue Q, Liu X, Russell P, et al. Evaluation of the binding performance of flavonoids to estrogen receptor alpha by autodock, autodock vina and surflex-dock. *Ecotoxicol Environ Saf*. 2022:233. doi:10.1016/j.ecoenv.2022.113323.
23. Quesada L, Areche C, Astudillo L, Gutiérrez M, Sepúlveda B, San-Martín A. Biological activity of isoflavonoids from Azorella madreporica. *Nat Prod Commun*. 2012;7(9):1187–1188. doi:10.1177/1934578x1200700921
24. Sweeney EE, Fan P, Jordan VC. Mechanisms underlying differential response to estrogen-induced apoptosis in long-term estrogen-deprived breast cancer cells. *Int J Oncol*. 2014;44(5):1529–1538. doi:10.3892/ijo.2014.2329
25. Saha Roy S, Vadlamudi RK. Role of estrogen receptor signaling in breast cancer metastasis. *Int J Breast Cancer*. 2012;2012:1–8. doi:10.1155/2012/654698
26. Jiang Z, Guo J, Shen J, Jin M, Xie S, Wang L. The role of estrogen receptor alpha in mediating chemoresistance in breast cancer cells. *J Exp Clin Cancer Res*. 2012;31(1). doi:10.1186/1756-9966-31-42
27. Akili Abd WR, Hardianto A, Latip J, Permana A, Herlina T. Virtual screening and ADMET prediction to uncover the potency of flavonoids from genus Erythrina as antibacterial agent through inhibition of bacterial ATPase DNA gyrase B. *Molecules*. 2023;28(24):8010. doi:10.3390/molecules28248010
28. Ferreira De Freitas R, Schapira M. A systematic analysis of atomic protein-ligand interactions in the PDB. *Medchemcomm*. 2017;8(10):1970–1981. doi:10.1039/c7md00381a
29. Li WM, Li XB, Sun SX, Liang J, Wang RL, Wang SQ. Agonist and antagonist recognition studies for oestrogen receptor by molecular dynamics simulation. *Mol Simul*. 2013;39(3):228–233. doi:10.1080/08927022.2012.717281
30. Sinyani A, Idowu K, Shunmugam L, Kumalo HM, Khan R. A molecular dynamics perspective into estrogen receptor inhibition by selective flavonoids as alternative therapeutic options. *J Biomol Struct Dyn*. 2023;41(9):4093–4105. doi:10.1080/07391102.2022.2062786
31. Furman C, Hao MH, Prajapati S, et al. Estrogen receptor covalent antagonists: the best is yet to come. *Cancer Res*. 2019;79(8):1740–1745. doi:10.1158/0008-5472.CAN-18-3634
32. Madriwala B, S BV, Jays J. Molecular docking study of hentriacontane for anticancer and antitubercular activity. *Int J Chem Res*. 2022; 1–4. doi:10.22159/ijcr.2022v6i4.208.
33. De Vivo M, Cavalli A. Recent advances in dynamic docking for drug discovery. *Wiley Interdiscip Rev Comput Mol Sci*. 2017;7(6). doi:10.1002/wcms.1320
34. Abdalla M, Eltayb WA, El-Arabey AA, Singh K, Jiang X. Molecular dynamic study of SARS-CoV-2 with various S protein mutations and their effect on thermodynamic properties. *Comput Biol Med*. 2022;141. doi:10.1016/j.compbiomed.2021.105025
35. Patel JM, Jeselsohn RM. Estrogen receptor alpha and ESR1 mutations in breast cancer. In *Advances in Experimental Medicine and Biology. Vol 1390*. Springer; 2022:171–194.
36. Ruff M, Gangloff M, Marie Wurtz J, Moras D. Estrogen receptor transcription and transactivation structure-function relationship in DNA- and ligand-binding domains of estrogen receptors. *Breast Cancer Res*. 2000;2(5). doi:10.1186/bcr80
37. Bruning JB, Parent AA, Gil G, et al. Coupling of receptor conformation and ligand orientation determine graded activity. *Nat Chem Biol*. 2010;6(11):837–843. doi:10.1038/nchembio.451
38. Kraichely DM, Sun J, Katzenellenbogen JA, Katzenellenbogen BS. Conformational changes and coactivator recruitment by novel ligands for estrogen receptor-α and estrogen receptor-β: correlations with biological character and distinct differences among SRC coactivator family members. *Endocrinology*. 2000;141(10):3534–3545. doi:10.1210/endo.141.10.7698
39. Ng HL, Kumar K, Duarte F, Pimentel AS, Paton RS. Simulations reveal increased fluctuations in estrogen receptor-alpha conformation upon antagonist binding. *J Mol Graph Model*. 2016;67:69. doi:10.1016/j.jmgm.2016.08.009
40. Ng HW, Zhang W, Shu M, et al. Competitive molecular docking approach for predicting estrogen receptor subtype α agonists and antagonists. *BMC Bioinf*. 2014;15(11). doi:10.1186/1471-2105-15-S11-S4
41. Sakkiah S, Selvaraj C, Hong H, et al. Elucidation of agonist and antagonist dynamic binding patterns in ER-α by integration of molecular docking, molecular dynamics simulations and quantum mechanical calculations. *Int J Mol Sci*. 2021;22(17):9371. doi:10.3390/ijms22179371
42. Nishinarizki V, Hardianto A, Gaffar S, Muchtaridi M, Herlina T. Virtual screening campaigns and ADMET evaluation to unlock the potency of flavonoids from Erythrina as 3CLpro SARS-COV-2 inhibitors. *J Appl Pharm Sci*. 2023;13(2). doi:10.7324/JAPS.2023.130209
43. Savva M, Paavola N, Kiser TH, Wright G, Jacknin G. On the origin of the apparent volume of distribution and its significance in pharmacokinetics. *J Biosci Med*. 2022;10(01):203–211. doi:10.4236/jbm.2022.101008